Journal of Applied Electrochemistry **31**: 839–844, 2001.

Kinetic study of 3,6-dimethylthieno[3,2-*b*]thiophene electropolymerisation

S.B. SAIDMAN[1,*], R.O. GARAY[2] and J.B. BESSONE[1]
[1]*Instituto de Ingeniería Electroquímica y Corrosión (INIEC), Universidad Nacional del Sur, Bahía Blanca, Argentina*
[2]*Instituto de Investigaciones en Química Orgánica (INIQO), Universidad Nacional del Sur, Bahía Blanca, Argentina*
*(*author for correspondence, e-mail: ssaidman@criba.edu.ar)*

Received 4 December 2000; accepted in revised form 4 April 2001

Key words: cyclic voltammetry, 3,6-dimethylthieno[3,2-*b*]thiophene, electropolymerisation, potential step

Abstract

A systematic investigation was carried out by means of cyclic voltammetry, chronoamperometry and chronopotentiometry on 3,6-dimethylthieno[3,2-*b*]thiophene (DMTT) electropolymerisation on vitreous carbon in acetonitrile (ACN) containing 0.1 M $LiClO_4$. The electrochemical doping–undoping process was reversible and the coulombic efficiency over a charge–discharge cycle was ca. 100%. The electropolymerisation mechanism was unchanged by the presence of methyl groups. When an aluminium electrode was used, poly(DMTT) deposition could only be performed in the potentiostatic mode. In this case, electropolymerisation hindered the pitting process on Al, which was initiated in the early stages of anodisation.

1. Introduction

Polymers with good cyclability and colour change upon electrochemical reaction have possible uses in rechargeable batteries and electrochromic displays. Thus, fused-ring systems containing thiophene units have been electropolymerized under various conditions due to their conducting, optical and catalytic properties [1].

Thienothiophenes are much easier to oxidise than thiophene itself due to the larger π-electron delocalisation in the fused-ring structure [2]. Hence, the corresponding polymers can be driven to a reduced state by setting the electrode potential to more negative values. Electropolymerisation of thieno[3,2-*b*]thiophene was reported by Danieli et al. [3]. Electrochemical characterisation by cyclic voltammetry showed that the polymer, which has low conductivity, could be repeatedly transformed between the doped and the undoped species. The polymer is expected to consist mainly of α,α'-linked units since α-substituted derivatives do not yield polymeric products [2]. The reactivity of the starting monomer, which is influenced by the substituents steric and electronic properties, affects the resulting polymer quality. Among others, alkyl groups are common substituents at the β-position of thiophene rings. The positively charged polymer chain is stabilised due to the inductive effect of the alkyl groups [1, 4]. Also, the 3,4-substitution in the thiophene ring facilitates the formation of linear polymer chains, which should lead to increased conjugation length, and also lowers the oxidation potential at which the monomer polymerises [5]. Thus, the substitution of the thieno[3,2-*b*]thiophene may result in new possibilities for the modification of the polymer properties. Consequently, we performed a systematic investigation by means of cyclic voltammetry, chronoamperometry and chronopotentiometry of 3,6-dimethyl thieno[3,2-*b*]thiophene (DMTT) electropolymerisation in acetonitrile (ACN) electrolyte.

There has been an increasing interest lately in the use of conducting polymers as anti-corrosion coatings. Therefore, a first attempt to deposit poly(DMTT) on aluminium was performed. In spite of the fact that aluminium is an electroactive metal and that anodic electropolymerisation thereon is consequently very difficult, polymer coatings have already been achieved from other monomer solutions in aqueous and non-aqueous electrolytes [6–10].

2. Experimental details

Vitreous carbon or aluminium (99.999%, Aldrich Chemical Company) rods embedded in a teflon holder with an exposed area of 0.070 cm^2 were used as working electrodes. The electrodes were polished with 1000 emery paper, 1 and 0.3 μm grit alumina suspensions, then cleaned with triple distilled water and wiped with filter paper. A monomer modified carbon paste electrode was also used. Carbon paste was prepared by hand mixing 1.00 g of graphite (Graphite extrapure, Merck), 0.4 ml of paraffin-oil (Uvasol, Merck) and 0.16 g of sodium dodecyl sulphate. The auxiliary electrode was a large Pt sheet. The reference electrode was an Ag/AgCl (Metrohm) with a standard potential of 0.100 V vs NHE

(The inner electrolyte was LiCl sat in EtOH and the outer was ACN/0.1 M $LiClO_4$). All experiments were performed in a 20 cm^3 Metrohm measuring cell.

DMTT, which was employed as the monomer for the electropolymerisation, was synthesised and purified following the method previously described by Choi et al. [11].

All measurements were performed in ACN (HPLC grade) with $LiClO_4$ (p.a.) as supporting electrolyte in a purified nitrogen gas saturated atmosphere at 25 °C.

Current–potential responses were obtained using a linear voltage sweep generator PAR model 175, a potentiostat–galvanostat PAR model 173 and HP 4007 B *x–y* recorder. A dual stage ISI DS 130 SEM and an EDAX 9600 quantitative energy dispersive analyser were used to examine the morphology and composition of the deposits.

IR spectra were recorded as potassium bromide (KBr) pellets using an IBM IR30-S FTIR spectrophotometer.

3. Results and discussion

3.1. *Electropolymerisation on vitreous carbon*

Figure 1 shows the cyclic voltammograms for the first, fifth, tenth and fifteenth cycles of a vitreous carbon electrode in a ACN + 0.1 M $LiClO_4$ solution containing (a) 10^{-3} M and 5×10^{-3} M DMTT, where the electrode potential is continuously swept at a rate of 0.05 V s^{-1} between −0.35 and 1.65 V. The same response was obtained by using a Pt electrode. During the first cycle an increase in the anodic current is observed at about 1.30 V following a Tafel behaviour (Figure 2). As expected, this potential is lower than the thieno[3,2-*b*]thiophene oxidation potential. An anodic peak appears behind the Tafel region and its peak current, $i_{p,I}$, shows a linear dependence on $v^{1/2}$ and is proportional to the monomer concentration, following the equation

$$(\log i_{p,I}/\log c_{DMTT}) = 1$$

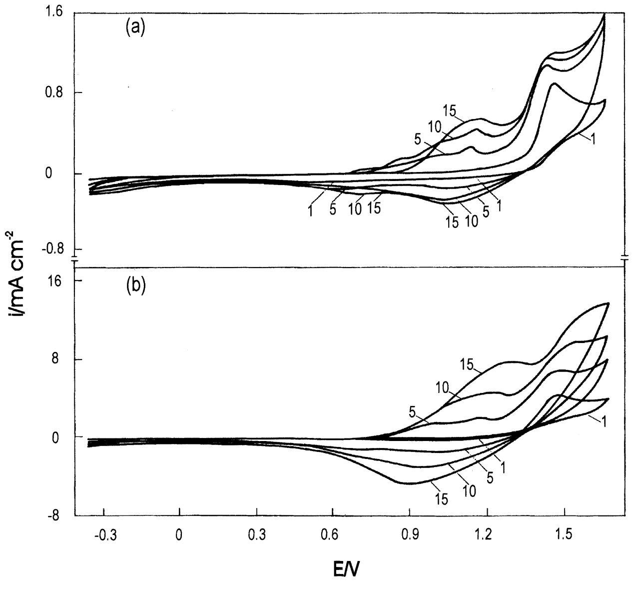

Fig. 1. Continuous cyclic voltammograms of DMTT in ACN + 0.1 M $LiClO_4$ solution of a vitreous carbon electrode. Scan rate: 0.05 V s^{-1}. (a) 10^{-3} M DMTT; (b) 5×10^{-3} M DMTT.

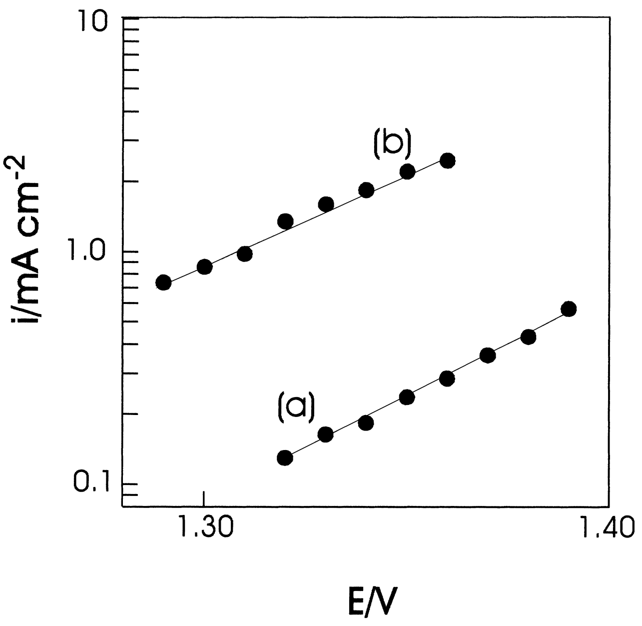

Fig. 2. Tafel plots taken from the first cycles of the potential sweeps such as those shown in Figure 1. (a) 10^{-3} M DMTT; (b) 5×10^{-3} M DMTT.

It is also observed that the anodic current tends to a limiting value when a rotating disk electrode, with rotation speeds up to 2000 rev min^{-1}, is used.

From the above results, it is concluded that the anodic reaction at the peak potential is controlled by the monomer diffusion in the solution. New reduction–oxidation waves also appear at potentials more negative than the potential at which the irreversible oxidation of the monomer takes place. The current in the cyclic voltammogram increases with each scan, indicating the build-up of electroactive polymeric products. This polymeric film shows a potential dependent change in colour typical of conducting polymers. Depending on the amount of charge passed, a violet to blue oxidised polymer film is deposited, while the neutral form varies from yellow to brown.

In the polymer oxidation process, the cyclic voltammograms show three anodic peaks with variable contributions as the film becomes thicker (Figure 1). Also, the two cathodic waves merge into one peak in the subsequent scans. A similar behaviour for polybithienyl was found by Zhang et al. [12], who suggested that the first cathodic peak represents the reduction of the oxidised oligomer and the second cathodic peak, at higher overpotentials, the reduction of the oxidised polybithienyl. In our case, the poly(DMTT) film changed from blue to yellow at the more negative peak. Therefore, the current peak at the more negative

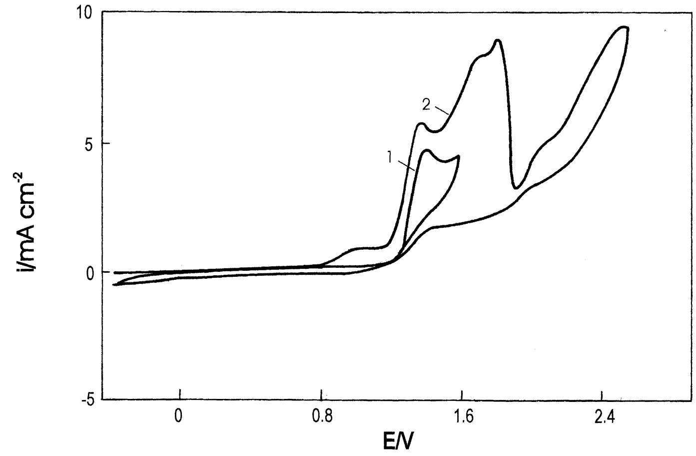

Fig. 3. Influence of increasing the anodic switching potential on the voltammograms of 10^{-3} M DMTT in ACN + 0.1 M $LiClO_4$ solution of a vitreous carbon electrode. Scan rate: 0.05 V s^{-1}.

potential corresponds to the reduction of the oxidised poly(DMTT). The growth rate starts to decrease around the tenth and the thirteenth potential cycles for 10^{-3} and 5×10^{-3} M DMTT concentrations, respectively. The slope of the initial portion of the anodic peak fits a linear potential/current relationship (Figure 1), indicating an increasing polymer resistance as the deposited charge increases. Extending the positive scan limit, a current peak associated with the overoxidation of poly(DMTT) is obtained, followed by the oxidation of the medium (Figure 3). Extending the negative scan limit to −2.50 V, no evidence of an n-doping process is obtained, as was observed for polythienothiophene [2].

The FTIR spectrum of a KBr pellet of the doped poly(DMTT) showed the typical pattern of the doped parent polythieno[3,2-*b*]thiophene [3], whose band contour is dominated by bands at 1170–1090 cm^{-1} corresponding to the perchlorate counter ion (Figure 4). In our case, very weak signals appears below 3000 cm^{-1} which correspond to the vibration mode of the methyl groups C–H bonds. However, the FTIR spectrum of the chemically (H_2O) undoped poly(DMTT) clearly showed the disappearance of the sharp aromatic CH stretch mode at 3094 cm^{-1} which is present in the monomer FTIR spectrum. Therefore, the lack of this vibration mode in the polymer indicates that the monomer is electrochemically coupled at positions 2 and 5. The methyl substitution is expected to give the polymer an increased solubility in organic solvents. However, all attempts to dissolve doped or undoped poly(DMTT) using a variety of solvents were unsuccessful. Therefore, a small amount of crosslinking cannot be ruled out. On the other hand, it is unlikely that the conformational disorder and reduced chain interaction, brought about by the introduction of the methyl groups in the main chain, would suffice to produce a soluble extended-rod polymer. The polymer can also be galvanostatically deposited and Figure 5 represents the chronopotentiometric response. For current densities lower than 0.1 mA cm^{-2}, and after a time delay, the potential rises to 1.30 V and then decreases to a value of about 1.22 V. The initial time delay is related to the fact that some time and an appropriate radical cation concentration are required to start the polymer nucleation, while the

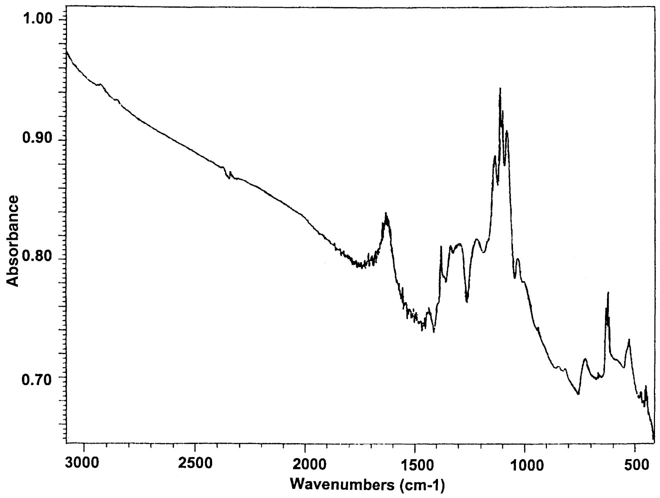

Fig. 4. FTIR spectrum of the doped polymer in KBr pellets.

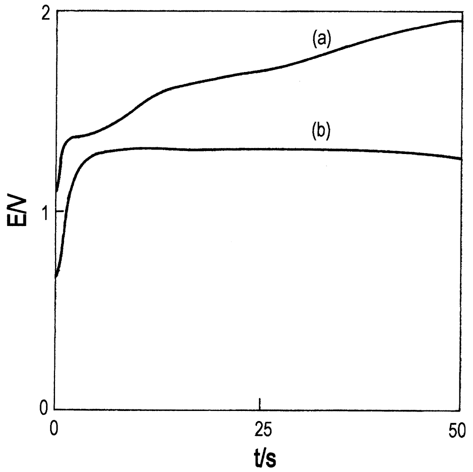

Fig. 5. Potential–time transient for the galvanostatic electropolymerisation of poly(DMTT) of a vitreous carbon electrode from 5 × 10^{-3} M DMTT and ACN + 0.1 M $LiClO_4$ solution at a current density of: (a) 0.5 mA cm^{-2}; (b) 0.1 mA cm^{-2}.

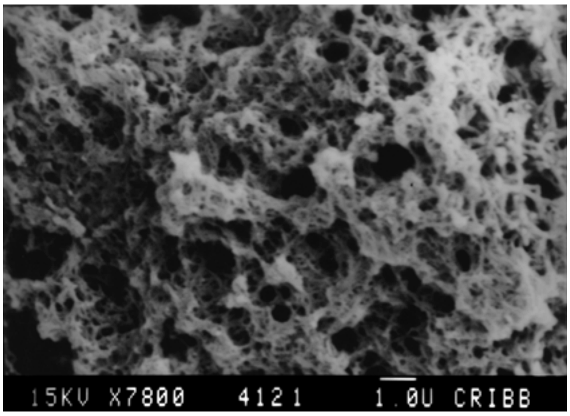

Fig. 6. SEM micrograph of the polymer obtained in ACN + 0.1 M $LiClO_4$ + 5 × 10^{-3} M DMTT after 250 s at 0.4 mA cm^{-2}.

potential decrease for longer deposition times can be attributed to the increase in the polymer surface area during the electropolymerisation. Under the above conditions, uniform and dark blue polymer films are deposited on the electrode. The deposited material can easily be scraped, as occurs with poly(thieno[3,2-*b*]thiophene). In contrast, the film generated at current densities higher than 0.1 mA cm^{-2} has very low adherence. In this case, we observed that the potential jumped to values higher than 2 V, that is to a potential region associated with the overoxidation of poly(DMTT), which will prevent normal polymer growth. Higher current densities must be applied in a solution with higher monomer concentrations to reach this degradation potential region. A SEM micrograph of the polymer obtained in 5 × 10^{-3} M DMTT after 250 s at 0.4 mA cm^{-2} shows a spongy film (Figure 6).

Current peaks decrease with the number of cycles when poly(DMTT) electrodes, formed by conventional voltammetry, are cycled in a monomer-free solution, indicating that the films are unstable in the background electrolyte. In contrast, galvanostatically formed films show good stability and it was therefore preferred to synthesis them by applying a constant current. Thus, several poly(DMTT) films were electrosynthesised on vitreous carbon at constant $i = 0.4$ mA cm^{-2} for 7 min from a 5 × 10^{-3} M DMTT solution. Polymer coated electrodes were rinsed with ACN to remove the monomer excess, transferred to a monomer-free electrolyte medium and cycled between −0.35 and 1.20 V at different sweep rates. Cyclic voltammograms show two anodic peaks at 0.74 (peak I) and 1.01 V (peak II) (Figure 7). It appears that the charge of peak I increases at the expense of that of peak II until a stable response is obtained. This behaviour may be attributed to structural rearrangement. The same peak pattern was present for a polymer generated in 10^{-3} M DMTT when the same charge during polymer growth is consumed (Figure 6b). Furthermore, the cathodic current defines two broad waves without any changes in the cyclic voltammogram. The films are quite stable and can be cycled for 4 h without evidence of decomposition. A linear relationship between the anodic peak current (peaks I and II) and the sweep rate was found when the electrodes were cycled at different sweep rates. This observation indicates that a reaction of surface localised material took place. The integrated charges under the oxidation and the reduction waves are very similar, thus the coulombic efficiency over a cycle of charge–discharge is ca. 100%. The oxidation degree of the oxidised polymer or the doping level of the anion in the film (d_{PDMTT}) may be calculated from

$$d_{PDMTT} = 2Q_{ox}/(Q - Q_{ox})$$

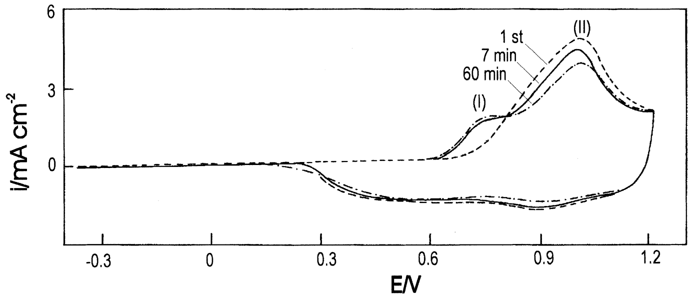

Fig. 7. Cyclic voltammograms of a poly(DMTT) film in an ACN + 0.1 M $LiClO_4$ solution. The film was made galvanostatically from a ACN + 5 × 10^{-3} M DMTT + 0.1 M $LiClO_4$ using 200 mC cm^{-2}. Scan rate: 0.05 V s^{-1}.

where Q_{ox} is the integrated charge under the oxidation peaks and Q is the charge consumed during polymer growth. A value of 29% was obtained when the polymer was grown galvanostatically ($Q = 200$ mC cm^{-2}). Assuming that the electropolymerisation reaction proceeds via an R–R mechanism, each monomer molecule loses 2.29 electrons and two protons in forming one oxidised repeating unit. The same value of doping level was obtained for a polymer grown in a 10^{-3} M DMTT solution at a current density lower than 0.1 mA cm^{-2} but also consuming 200 mC cm^{-2}.

In spite of the fact that the redox process is not electrochemically reversible, the electrochemical doping–undoping process is reversible because the polymer may repeatedly be reduced to the neutral state and oxidised to the conducting state. Furthermore, it was found that the anodic and cathodic waves are very broad. Similar results were reported for poly(dithienothiophene) by Biserni et al. [13], who suggested that the doping–undoping process for this polymer is complex due to polymeric chain reorganisation. A more uniform distribution of polymer chains can be expected to yield a much sharper peak. Probably, as in the case of poly(thieno[3,2-*b*]thiophene), poly(DMTT) also lacks a high degree of structural homogeneity, despite the more regularly α,α'-linked monomer units and a much lower degree of hydrogen saturation of the film.

3.2. *Electropolymerisation on aluminium*

In an attempt to produce electropolymerisation of DMTT on Al, potentiodynamic polarisation was carried out under the same conditions described for the vitreous carbon electrode. Only highly localised electrodeposits of polymer were produced under these conditions. The same result was obtained applying a current step. It is known that perchlorate ions produce pits on Al [14] and that complexes of Al(III) with CN group of acetonitrile can occur [15]. However, better results were obtained when the Al electrode was polarised in the potentiostatic mode. The current transient recorded in a monomer-free solution (Figure 8, full line) shows that the current initially decreases to a minimum and later increases to reach a maximum. Finally, current oscillations appear while the current rises continually. This current behaviour may comprise the contribution of the current related to the passive layer growth and the current related to the nucleation and growth of pits. The current transient recorded in the presence of monomer in solution (Figure 8, dashed line) suggests that nucleation of pits occurs together with the passive layer formation. But, immediately after the DMTT starts to be oxidised, its electropolymerisation begins to hinder the progress of the pitting process. Finally, polymerisation products cover the initially pitted surface and the current density tends to a steady state value. After a few seconds, a homogeneous and dark film is obtained.

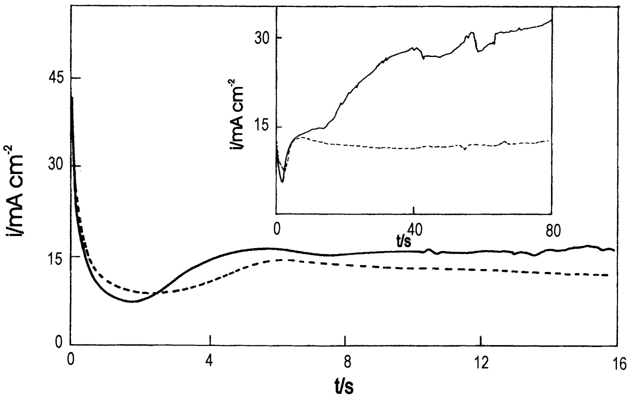

Fig. 8. Chronoamperograms obtained on aluminium at a constant potential of 1.65 V in ACN + 0.1 M $LiClO_4$ solution (——) without and (- - - - -) with 5×10^{-3} M DMTT. The variation of *i* at longer times is also included.

4. Conclusions

The deposition of poly(DMTT) onto vitreous carbon from an ACN solution occurs under electron transfer control at low polarisation potential while at high polarisation potentials it is controlled by the monomer diffusion. More positive potentials result in the anodic overoxidation of poly(DMTT).

The polymer generated under galvanostatic conditions has better stability than that formed under potentiodynamic conditions. The electrochemical doping–undoping process is reversible and the coulombic efficiency over a cycle of charge–discharge is ca. 100%. Each monomer molecule loses 2.29 electrons and two protons in forming one oxidised repeating unit. The electropolymerisation mechanism of poly(thieno[3,2-*b*]thiophene) is not changed by the presence of the methyl groups. Poly(DMTT) deposition on aluminium can only be performed in the potentiostatic mode. Electropolymerisation hinders the progress of the pitting process on Al, initiated in the early stages of anodisation.

Acknowledgements

Fundación Antorchas and Consejo Nacional de Investigaciones Científicas y Técnicas (PEI no. 0233797) are gratefully acknowledged for financial support.

References

1. G. Zotti, In: Handbook of Organic Conducting Molecules and Polymers, H.S. Nalwa (ed.), Vol. 2, Wiley, New York, 1997, p. 137.
2. R. Lazzaroni, A. De Pryck, Ch. Debaisieux, J. Riga, J. Verbist, J.L. Bredas, J. Delhalle and J.M. André, *Synth. Met.* **21** (1987) 189.
3. R. Danieli, C. Taliani, R. Zamboni, G. Giro, M. Biserni, M. Mastragostino and A. Testoni, *Synth. Met.* **13** (1986) 325.
4. R.J. Waltman and J. Bargon, *Can. J. Chem.* **64** (1986) 76.
5. C. Kvarnstrom, H. Neugebauer, S. Blomquist, H.J. Ahonen, J. Kankare and A. Ivaska, *Electrochim. Acta* **44** (1999) 2739.

6. P. Hülser and F. Beck, *J. Appl. Electrochem.* **20** (1990) 596.
7. F. Beck and P. Hülser, *J. Electroanal. Chem.* **289** (1990) 159.
8. Z. Mekhalif, J. Delhalle, P. Lang, F. Garnier and R. Caudano, *J. Electrochem. Soc.* **146** (1999) 2913.
9. S. Aeiyach, E. Bazzaoui and P.C. Lacaze, *J. Electroanal. Chem.* **434** (1997) 153.
10. N. Sakmeche, J.J. Aaron, S. Aeiyach and P.C. Lacaze, *Electrochim. Acta* **45** (2000) 1921.
11. K.S. Choi, K. Sawada, H. Dong, M. Hoshino and J. Nakayama, *Heterocycles* **38** (1994) 143.
12. W. Zhang, W. Plieth and G. Koßmehl, *Electrochim. Acta* **42** (1997) 1653.
13. M. Biserni, A. Marinangeli and M. Mastragostino, *J. Eletrochem. Soc.* **132** (1985) 1597.
14. J.R. Galvele and S.M.De Micheli, *Corros. Sci.* **10** (1970) 795.
15. L. Bai and B.E. Conway, *J. Electrochem. Soc.* **137** (1990) 3737.